Research Article | Vol. 25, No. 10 | 15 May 2017 | OPTICS EXPRESS 11365

Optics EXPRESS

Measurement and control of the sideband to carrier ratio of an electro-optic modulator used in atom interferometers

LEI ZHU,[1,2,4] JIAQI ZHONG,[1,4,6] XI CHEN,[1,4] HONGWEI SONG,[1,3] XIAOWEI ZHANG,[1,2,4] BIAO TANG,[1,4] FEN GAO,[1,5] JIN WANG,[1,4,7] AND MINGSHENG ZHAN[1,4,8]

[1]*State Key Laboratory of Magnetic Resonance and Atomic and Molecular Physics, Wuhan Institute of Physics and Mathematics, Chinese Academy of Sciences - Wuhan National Laboratory for Optoelectronics, Wuhan 430071, China*
[2]*School of Physics, University of Chinese Academy of Sciences, Beijing 100049, China*
[3]*School of Optical and Electronic Information, Huazhong University of Science and Technology, Wuhan 430074, China*
[4]*Center for Cold Atom Physics, Chinese Academy of Sciences, Wuhan 430071, China*
[5]*School of Physics, Huazhong University of Science and Technology, Wuhan 430074, China*
[6]*jqzhong@wipm.ac.cn*
[7]*wangjin@wipm.ac.cn*
[8]*mszhan@wipm.ac.cn*

Abstract: The sideband and carrier of an electro-optic modulator (EOM) are usually used as Raman lasers in atom interferometry. To eliminate AC-Stark shift in atom interferometry, the stability of sideband to carrier ratio (SCR) is of great significance. We present a beating method to accurately measure and control the SCR. The influence of imperfect frequency response of the beating system is avoided by chirping the reference laser with half chirping rate of the modulation frequency. Making use of this method, we performed a SCR locking by feedback to the modulation depth. The locked SCRs' variation is averaged to be less than 0.1% within 20 MHz chirping span, and the according error for gravity measurement with 180 ms free evolution time is $6.2\times10^{-11}g$. Thus both the SCR variation and the estimated gravity measurement error are reduced by about 2 orders. This work may provide hints to other EOM involving experiments.

OCIS codes: (020.1335) Atom optics; (020.6580) Stark effect; (140.3550) Lasers, Raman.

References and links

1. M. Kasevich, and S. Chu, "Atomic interferometry using stimulated Raman transitions," Phys. Rev. Lett. **67**(2), 181–184(1991).
2. M. G. Tarallo, T. Mazzoni, N. Poli, D. V. Sutyrin, X. Zhang, and G. M. Tino, "Test of Einstein equivalence principle for 0-Spin and half-integer-spin atoms: search for spin-gravity coupling effects," Phys. Rev. Lett. **113**(2), 023005(2014).
3. L. Zhou, S. T. Long, B. Tang, X. Chen, F. Gao, W. C. Peng, W. T. Duan, J. Q. Zhong, Z. Y. Xiong, J. Wang, Y. Z. Zhang, and M. S. Zhan, "Test of equivalence principle at 10^{-8} level by a dual-species double-diffraction Raman atom interferometer," Phys. Rev. Lett. **115**(1), 013004(2015).
4. H. Müller, A. Peters, and S Chu, " A precision measurement of the gravitional redshift by the interference of matter waves," Nature **463**(7283), 926–929(2010).
5. H. Müller, A. Peters, and S Chu, "Atom gravimeters and gravitational redshift," Nature **463**, 09340 (2010).
6. Wolfgang P Schleich, Daniel M Greeenberger, and Ernst M Rasel, "A representation-free description of Kasevich-Chu interferometer: a resolution of redshift controversy," New J. Phys **15**, 013007 (2013).
7. G. Rosi, F. Sorrentino, L. Cacciapuoti, M. Prevedeli, and G. M. Tino, "Precision measurement of the Newtonian gravitational constant using cold atoms," Nature **510**(7506), 518–521(2015)
8. A. Peters, K. Y. Chung, and S. Chu, "High-precision gravity measurements using atom interferometry," Metrologia **38**(1), 25–61(2001).
9. Z. K. Hu, B. L. Sun, X. C. Duan, M. K. Zhou, L. L. Chen, S. Zhan, Q. Z. Zhang, and J. Luo, "Demonstration of an ultrahigh-sensitivity atom-interferometry absolute gravimeter," Phys. Rev. A **88**(4), 043610(2013).

#287063 https://doi.org/10.1364/OE.25.011365
Journal © 2017 Received 20 Feb 2017; revised 19 Apr 2017; accepted 4 May 2017; published 8 May 2017

Optics EXPRESS

10. J. M. McGuirk, G. T. Foster, J. B. Fixer, M. J. Snadden, and M. A. Kasevich, "Sensitive absolute-gravity gradiometry using atom interferometry," Phys. Rev. A **65**(3), 033608(2002).
11. F. Sorrentino, A. Bertoldi, Q. Bodart, L. Cacciapuoti, M. de Angelis, Y.-H. Lien, M. Prevedelli, G. Rosi and G. M. Tino, "Simultaneous measurement of gravity acceleration and gravity gradient with an atom interferometer," Appl. Phys. Lett. **101**(11), 114106(2012).
12. B. Canuel, F. Leduc, D. Holleville, A. Gauguet, J. Fils, A. Virdis, A. Clairon, N. Dimarcq, Ch. J. Borde, A. Landragin, and P. Bouyer, "Six-axis inertial sensor using cold-atom interferometry," Phys. Rev. Lett. **97**(1), 010402(2006).
13. D. S. Durfee, Y. K. Shaham, and M. A. Kasevich, "Long-term stability of an area-reversible atom-interferometer Sagnac gyroscope," Phys. Rev. Lett. **97**(24), 240801(2006).
14. M. Schmidt, M. Prevedelli, A. Giorgini, G. M. Tino, and A. Peters, "A portable laser system for high-precision atom interferometry experiments," Appl. Phys. B **102**(1), 11–18(2011).
15. L. Zhou, Z. Y. Xiong, W. Yang, B. Tang, W. C. Peng, Y. B. Wang, P. Xu, J. Wang, and M. S. Zhan, " Measurement of local gravity via a cold atom interferometer," Chin. Phys. Lett. **28**(1), 013701(2011).
16. K. Wang, Z. W. Yao, R. B. Li, S. B. Lu, X. Chen, J. Wang, and M. S. Zhan, "Hybrid wide-band, low-phase-noise scheme for Raman lasers in atom interferometry by integrating an acousto-optic modulator and a feedback loop," Appl. Opt. **55**(5), 989–992(2016).
17. I. Dotsenko, W. Alt, S. Kuhr, D. Schrader, M. Müller, Y. Miroshnychenko, V. Gomer, A. Rauschenbeutel, and D. Meschede, "Application of electro-optically generated light fields for Raman spectroscopy of trapped cesium atoms," Appl. Phys. B **78**(6), 711–717(2004).
18. R. Geiger, V. Menoret, G. Stern, N. Zahzam, P. Cheinet, B. Battelier, A. Villing, F. Moron, M. Lours, Y. Bidel, A. Bresson, A. Landragin, and P. Bouyer, "Detecting inertial effects with airborne matter-wave interferometry," Nat. Commun. **2**(1), 474 (2011).
19. O. Carraz, F. Lienhart, R. Charriere, M. Cadoret, N. Zahzam, Y. Bidel, and A. Bresson, "Compact and robust laser system for onboard atom interferometry," Appl. Phys. B **97**(2), 405(2009).
20. Abramowitz, and Stegun, Handbook of Mathematical Functions With Formulas, Graphs, and Mathematical Tables (Dover, 1965).
21. D. A. Steck,"Rubidium 85 D Line Data," http://steck.us/alkalidata (2013).
22. D. S. Weiss, B. C. Young, and S.Chu, "Precision measurement of $\hbar/m_{Cs}$ based on photon recoil using laser-cooled atoms and atomic interferometry," Appl. Phys. B **59**(3), 217–256(1994).

1. Introduction

In recent years, atom interferometers (AIs) [1] have played an important role in both fundamental physics and application fields, including test of equivalence principle [2, 3], measurement of gravitational redshift [4–6], determination of Newton's gravitational constant [7], measurement of gravity [8, 9], gravity gradient [10, 11] and rotation of the Earth [12, 13]. The stimulated Raman transition is the key technique of AIs, two counterpropagating Raman lasers with the frequency difference equalling to the spacing between ground states of atoms are employed to split, redirect, and recombine atom wave-packets. Several methods are used to generate Raman lasers, including optical phase-locked loops [14], multi-passed high frequency acousto-optic modulation [15, 16] and electro-optic phase modulation [17–19]. In the electro-optic modulation method, the sidebands and the carrier come from the same source and they are never spatially separated, that brings a high immunity to frequency noise, temperature fluctuation and mechanical vibration. Fiber-based electro-optic modulators (FEOMs) have low half-wave voltage V_π and compact size, they are widely used in newly developed atom interferometers.

For AI-based precision measurement, AC-Stark shift and Doppler shift are two major noise and error sources. AC-Stark shifts, which are caused by the components of Raman laser pair, decrease the fringe contrast and increase measurement error. To cancel the AC-Stark shifts, the intensity ratio of these components has to be adjusted and controlled accurately. For atom interferometers with vertical configuration, such as atom gravimeters, the atoms experience a long time free-fall. To accurately chirp the frequency of Raman lasers is necessary for compensating the gravity induced Doppler shift, and both the AC-Stark shift and the Doppler shift should be compensated simultaneously during the whole process of coherent manipulation of atoms.

Optics EXPRESS

A Febry-Perot etalon can be easily employed to measure the sideband-carrier ratio (SCR) of FEOM. However, the laser's high frequency intensity noise brings spurious fluctuation to the SCR signal, and the cavity's susceptibility to environmental factors (i.e. vibration and temperature fluctuation), to some extent, restricts its application in practical atom sensors. In this article, we propose and realize an accurate measurement and control of an FEOM's sideband-carrier ratio (SCR) by beating the sideband and carrier with a reference laser. In order to decrease the influence of frequency response character of measurement system, the frequency difference between two beating signals is fixed to a small value by chirping the reference beam with a rate of the half value of FEOM's modulation frequency. We found that during the Doppler compensation chirping, the SCR of the FEOM varies seriously even if the power of the driving microwave is fixed, and the corresponding AC-Stark shift induces a large error in gravity measurement. Then we performed a locking control of SCR for a sequence of Raman laser pulses during one frequency sweep by feedbacks to the modulation depth, then both the SCR variation and the corresponding measurement error are reduced markedly.

2. Principle of SCR measurement

When a laser beam is modulated by an electro-optic modulator (EOM), the relative intensity of the sideband is a Bessel expansion [20]

$$E = E_0 \sum_{n=0}^{\infty} J_n(\beta) e^{i((\omega+n\delta)t+\phi_\omega+n\phi_\delta)} + C.C. \tag{1}$$

where, E_0 is the electric field amplitude of incident light, ω is the frequency, δ is the modulation frequency of the EOM, β is the modulation depth, ϕ_ω and ϕ_δ are the initial phases of the incident light and the modulation microwave, respectively. Several sidebands are generated with frequencies of $\pm\, n\delta$ separated from the carrier (n = 1, 2, ...corresponding to the sideband order).

The relative strengths of all sidebands and carrier can be represented by $J_n(\beta)$, where $\beta \sim \pi V/V_\pi(\delta)$, V is the amplitude of the modulation microwave, and $V_\pi(\delta)$ is the half-wave voltage. The value of $V_\pi(\delta)$ depends on δ due to the effects of bandwidth, acoustic resonance, frequency-dependent loss, etc.

Since sidebands and carrier overlap in optical path, it is difficult to perform independent measurements for each component. Here we propose a frequency beating method to measure SCR by introducing a reference laser.

Considering the simple beating case of two light beams a and b, the light fields are expressed as

$$E_a = A_a \cos(\omega_a t + \phi_a) \tag{2}$$

$$E_b = A_b \cos(\omega_b t + \phi_b) \tag{3}$$

where, $A_{a,b}$, $\omega_{a,b}$ and $\phi_{a,b}$ represent the amplitude, frequency and phase of the light fields, respectively.

Ignoring the DC and high frequency terms, the power of the output beating signal

$$P \propto \eta(\Delta_\omega) A_a^2 A_b^2 \propto \eta(\Delta_\omega) I_a I_b \tag{4}$$

where, I_a and I_b are the intensities of the two incident lights, respectively, $\eta(\Delta_\omega)$ is the detection efficiency, and Δ_ω ($\Delta_\omega = |\omega_a\text{-}\omega_b|$) is the frequency of the beating signal.

For the case that a reference laser beats with the carrier and the +1 sideband at the same time, we get two beating signals with the frequencies $\Delta_{ref,0} = |\omega_0 - \omega_{ref}|$ and $\Delta_{ref,+1} = |\omega_0 + \delta - \omega_{ref}|$, respectively, where, ω_0 is the frequency of the carrier, ω_{ref} is the frequency of the

Optics EXPRESS

reference laser and δ is equal to the frequency of the microwave applied to the EOM. According to Eq. (4), the powers of the two beating signals $P_{ref,0}$ and $P_{ref,+1}$ are written as

$$P_{ref,0} \propto \eta(\Delta_{ref,0}) \cdot I_{ref} \cdot I_0 \tag{5}$$

$$P_{ref,+1} \propto \eta(\Delta_{ref,+1}) \cdot I_{ref} \cdot I_{+1} \tag{6}$$

where, I_{ref}, I_0 and I_{+1} represent the intensities of the reference laser, the carrier and the +1 sideband, respectively. The *SCR* is

$$SCR_{+1,0} = \frac{I_{+1}}{I_0} = \frac{P_{ref,+1}}{P_{ref,0}} \cdot \frac{\eta(\Delta_{ref,0})}{\eta(\Delta_{ref,+1})} \tag{7}$$

$\eta(\Delta_\omega)$ is a complex function of the beating frequency, and it is determined by the frequency response characteristic of the measurement system. However, if we set ω_{ref} approximately in the middle value of the frequencies of carrier and +1 sideband, that is

$$|\omega_0 - \omega_{ref}| \approx |\omega_0 + \delta - \omega_{ref}| \tag{8}$$

and then

$$SCR_{+1,0} \approx \frac{P_{ref,+1}}{P_{ref,0}} \tag{9}$$

As mentioned above, during the measurement of the SCR, we need only synchronously chirp ω_{ref} with half chirping rate of δ to satisfy the Eq. (8) and Eq. (9), thus the measurement of SCR is easily performed by the relative power of the two beating signals recorded by a frequency spectrum analyzer (FSA), and we need not to know the exact value of $\eta(\Delta_\omega)$.

3. Experimental setup

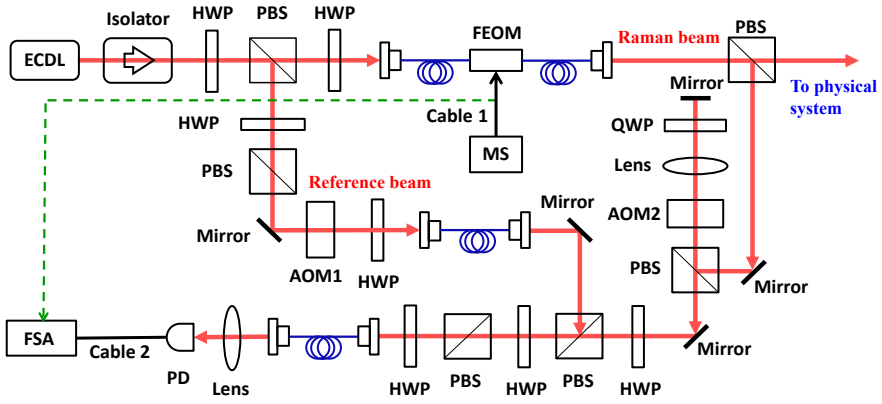

Fig. 1. Schematic diagram of the experimental setup. ECDL: external cavity diode laser; HWP: half-wave plate; QWP: quater-wave plate; FEOM: fiber based electro-optic modulator; AOM: acoustic-optic modulator; PBS: polarization beam splitter; MS: microwave source; PD: photodetector; FSA: frequency spectrum analyzer.

The schematic diagram of experimental setup for the SCR measurement is shown in Fig. 1. The output of an external cavity diode laser (ECDL, TOPTICA DL pro) is splitted into

Optics EXPRESS

two beams. One beam is phase modulated by an FEOM (Eospace PM-0K5-10), the driving microwave source (MS, Agilent E4433B) is operated at $\delta\sim3$ GHz, which is equal to the spacing between two ground states of ^{85}Rb. A series of sidebands, which have frequency spacing equalling to the operating frequency of the MS, are generated as Raman beams for coherently manipulating atoms. The other beam's frequency is shifted by a high frequency acoustic-optic modulator (AOM1, Brimrose GPF-1500) operating at $\gamma\sim1.5$ GHz, it is used as the reference beam. A half wave plate (HWP) and a polarization beam splitter (PBS2) are placed in front of AOM1 for adjusting the intensity of the reference beam. Two beams are recombined by PBS4 and detected by a PD (New Focus 1577-A-M). Finally, the beating signal is recorded by an FSA (Agilent N9030A). To identify the stray signal caused by AOM1's driving source, the frequencies of all components in Raman beams are shifted by AOM2 which is driven by a 80 MHz RF signal source and works with double-pass configuration, thus the beating signal between the reference beam and carrier is different from the driving source of AOM1.

4. Accurate measurement and control of SCR

4.1. Calibration of microwave transmission loss

According to Eq. (1), the SCR varies with β, which is dominantly determined by the microwave power applied to the EOM. To reduce the influence due to the variation of microwave power, we investigated the dependence of output frequency of EOM on the power of driving microwave when the output power of MS is fixed. As is shown by green dashed line in Fig. 1, the Cable 1 is disconnected from FEOM and connected to FSA. The output power of MS is set as 10 dBm, and δ is scanned from 3.025 GHz to 3.045 GHz with a step of 2 MHz. The microwave power is measured by the FSA. Due to the transmission loss of the cable and the connectors, the power attenuation is about 4.5 dB and the peak-valley (P-V) fluctuation is 0.8%. The dependence of the microwave power on δ is shown in Fig. 2, the microwave power is calibrated and fixed at 10 dBm by adjusting the MS.

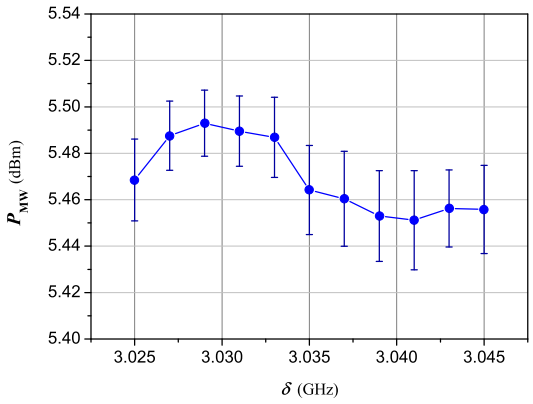

Fig. 2. Dependence of the microwave power on δ. The power in MS side is fixed at 10 dBm and each point is the average of ten measurements, and the error bars denote the standard deviation of the samples.

4.2. Measurement of SCR

The frequencies of the two laser beams are shown in Fig. 3. According to Section 2 and Eq. (8), when the Raman beam is modulated by the FEOM operating δ = 3.000 GHz and its frequency is shifted by AOM2 by -160 MHz, the frequency of the reference beam is blue shifted by γ =

Optics EXPRESS

1.341 GHz by AOM1, we observed two beating signals with the frequencies of 1.499 GHz and 1.501 GHz, respectively. Since the frequency difference between two signals is only 2 MHz, the detection efficiencies $\eta(\Delta_\omega)$ of the two signals can be considered as the same and the Eq. (9) is satisfied. During the measurement of SCR, the frequency of AOM1, γ, is chirped at half chirp rate of δ, e.g. γ = 1.342 GHz for δ = 3.002 GHz, thus the frequency difference between the two beating signals is fixed at 2 MHz.

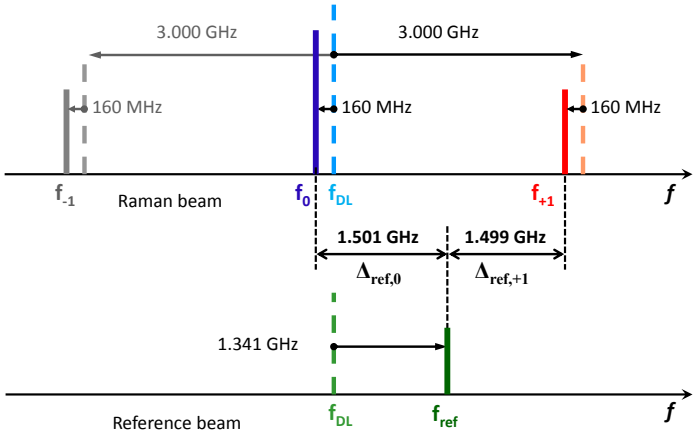

Fig. 3. The frequencies of Raman beam and reference beam. f_{DL}: the initial frequency of the ECDL; $f_{0,\pm1}$: the frequencies of the carrier and the ±1 order sidebands; f_{ref}: the frequency of the reference beam; $\Delta_{ref,0}$ and $\Delta_{ref,+1}$ are the frequencies of the two beating signals.

In the actual experiment, we scanned the value of δ from 3.025 GHz to 3.045 GHz, while the value of γ was synchronously scanned from 1.3535 GHz to 1.3635 GHz, the step intervals were 2 MHz and 1 MHz, respectively. The SNRs of both signals exceed 1000:1. The frequency dependence of SCR is shown in Fig. 4, the P-V variation is 10.7% within a span of 20 MHz. To evaluate the corresponding phase shift in the atom interferometer, we fit the data by least squares polynomial, the RMS of the fitting residuals is 5×10^{-4}.

4.3. *Influence of the reference beam intensity*

When δ = 3.025 GHz and γ = 1.3535 GHz, the powers of Raman beam and reference beam are measured as 120 μW and 4.5 μW, respectively. When γ is scanned from 1.3535 GHz to 1.3635 GHz, the diffraction angle of AOM1 changes, then the power of reference beam decreases from 4.5 μW to 2.5 μW due to the decrease of the fiber coupling efficiency. In order to study the influence of the intensity variation of the reference beam, we manually scan the power of the reference beam from 2.5 μW to 4.5 μW when δ = 3.035 GHz and γ = 1.3535 GHz. As is shown in Fig. 5, the variation of SCR is less than 0.5%, which is negligible and is coincide with theoretical prediction by Eq. (7).

4.4. *Closed loop control of SCR*

To eliminate the fringe phase shift induced by the variation of SCR during the frequency chirping, we performed a "closed loop" SCR locking by applying a proportional feedback to the output power of the FEOM's driving microwave (P_{MS}). As is shown in Fig. 6(a), in accordance

Optics EXPRESS

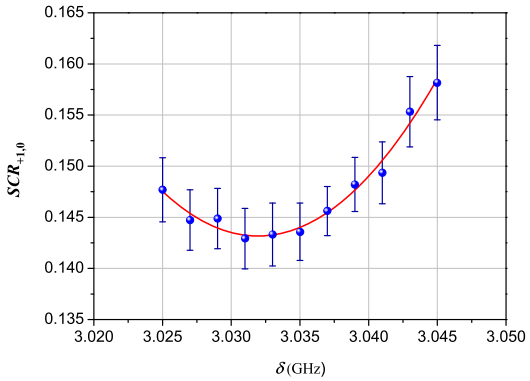

Fig. 4. Frequency dependence of SCR. Each point is the average of ten measurements, the error bars denote the standard deviation of the samples, and the red line is the polynomial fitting of the SCR.

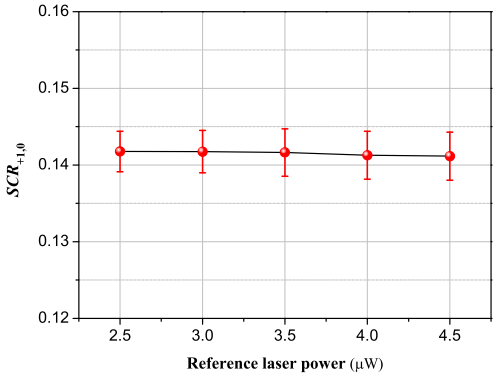

Fig. 5. SCR varies 0.5% when the power of the reference beam varies from 4.5 μW to 2.5 μW, this also agrees with the theory that the absolute power of the reference beam will not affect the measurement. Each point is the average of ten measurements and the error bars denote the standard deviation of measurements.

Optics EXPRESS

with theoretical prediction, to keep the SCR as a constant, the corresponding $P_{MS}(\delta)$ curve shows a very good complementary relationship with the measured SCR curve in Fig. 4. Thus we wrote a Labview (NI) program based on NI Compact RIO system (NI cRIO-9039 controller, sbRIO-9403 and sbRIO-9269 modules) to implement a proportional negative feedback. The FSA was connected with the system through a USB port and the measurement data can be transported in about 100 ms. Including subsequent Lorenz fitting and calculation, the feedback can be accomplished within 140 ms. We swept the frequency of the microwave source from 3.025 GHz to 3.045 GHz with 5 steps, the time interval is 180 ms, which is approximately in accordance with the gravity induced chirping rate 25 MHz/s. For an atom gravimeter (simply release type or fountain type) with the free evolution time T = 180 ms, 3 successive steps of the 5 are employed. When the feedback is switched on, the mean standard deviation of the 5 corresponding SCR within one sweep is decreased to be less than 1%, and the variation of the 5 averaged values is within 0.1%. The result is also shown in Fig. 6(a), the standard deviations of each data point , shown as the error bars, are also less than 1%. The allan deviation of SCR in free running mode and locking mode are compared in Fig. 6(b), the long-term drift is surpressed as well by the locking loop.

As is shown in 4.3, the SCR signal in this system is immune to the intensity fluctuation of the reference beam. And being different from AOM, the output sidebands and the carrier of FEOM are not spatially separated. Thus, the laser intensity variations of the sidebands and the carrier caused by the mechanical instability (e.g. the fluctuation of the fiber coupling efficiencies) are common mode rejected. Therefore, the short-term electrical noises, from the MS, FSA or the cables, are more likely to be the major limiting factors to our SCR measurement and control system with the precision 1%.

To test the effect of the feedback, we measured the atom's resonance frequency both in free running and locking mode of SCR. The experiment was carried out in a 34cm atom fountain, laser cooled ^{85}Rb atoms were prepared to $5^2S_{1/2}$ F = 2, m_F = 0 by a microwave pulse and a blowing away laser pulse after launching. Then 180 ms before the atoms reaching the apogee, a Raman laser pulse derived from the FEOM was switched on and finally the atoms transferred to F = 3, m_F = 0 were detected when they falled back to the detection region. Scanning the frequency of the microwave source shot by shot, the Raman transition resonance frequency can be evaluated by fitting the transition amplitude-frequency curve. We measured the resonance frequency about 50 times when the FEOM was operated in free running mode and SCR locking mode, respectively. As is shown in Fig. 7, the standard deviation was decreased from 2.4 kHz to 1.0 kHz after the feedback was switched on.

5. Reduction of the measurement error of atom gravimeter by feedback control of SCR

During the gravity measurement using atom interferometers, the frequency difference between Raman lasers is chirped to compensate Doppler shift. The AC-Stark shift caused by the unstable SCR is one of the error sources.

For atom gravimeters using ^{85}Rb atoms, the frequency of the Raman seed laser is locked to the red side of the $5^2S_{1/2}$ F = 3 $\rightarrow$ $5^2P_{3/2}$ transition with the detuning Δ. As is shown in Fig. 8, the Raman lasers are reflected by a mirror, thus a series of counter-propagating Raman laser pairs are generated. The AC-Stark shift of Raman resonance frequency caused by the carrier ($k = 0$), the ±1 order sidebands ($k = \pm1$) and the reflected components ($k = 0', \pm1'$) are

Optics EXPRESS

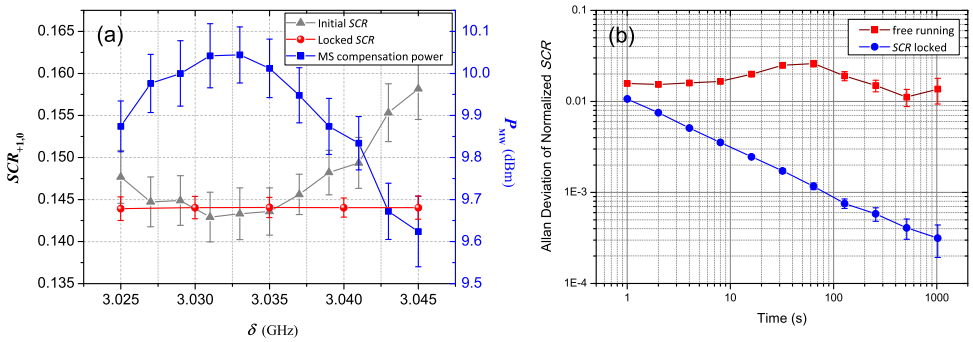

Fig. 6. (a): The grey triangle squares are SCR values versus δ, which is as same as shown in Fig. 4. The blue squares are the compensation powers of the FEOM's driving source, and the red dots are the remeasured SCR after the feedback is switched on. The error bars denote the standard deviation of measurements. (b): Allan Deviation of Normalized SCR in free running mode and SCR locking mode, respectively.

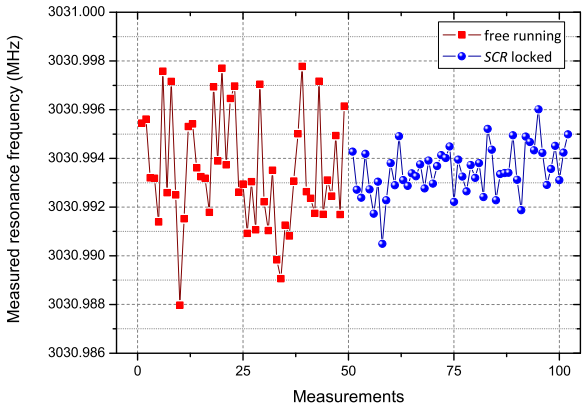

Fig. 7. Measurement of the resonance frequency in free running mode and SCR locking mode, respectively. The standard deviations of the measured frequency in free running mode and SCR locked mode are evaluated to be 2.4 kHz and 1.0 kHz.

Optics EXPRESS

expressed as

$$\delta^{AC} = \sum_{F',k} \frac{\Omega^2_{F=2,F',k}}{16\pi^2 \delta^{v}_{F=2,F',k}} - \sum_{F',k} \frac{\Omega^2_{F=3,F',k}}{16\pi^2 \delta^{v}_{F=3,F',k}}, \quad (F' = 1,2,3,4;\ k = -1,0,+1,-1',0',+1') \tag{10}$$

where, $\Omega_{F,F',k}$ is Rabi frequency, and $\delta^{v}_{F,F',k}$ is the detuning to the given transition.

$$\Omega_{F,F',k} = \frac{A_k(\boldsymbol{r})\langle F', M_F = 1|e\boldsymbol{r}|F, M_F = 0\rangle}{\hbar} \tag{11}$$

$$\delta^{v}_{F,F',k} = \Delta + \delta^{hfs}_{F'} \tag{12}$$

where, $A_k(\boldsymbol{r})$ is the amplitude of the electric field of the given Raman laser pair, and $\Omega_{F,F',k}$ can be calculated based on the D line data of ^{85}Rb [21], $\delta^{hfs}_{F'}$ is the hyperfine splitting of $5^2P_{3/2}$ states.

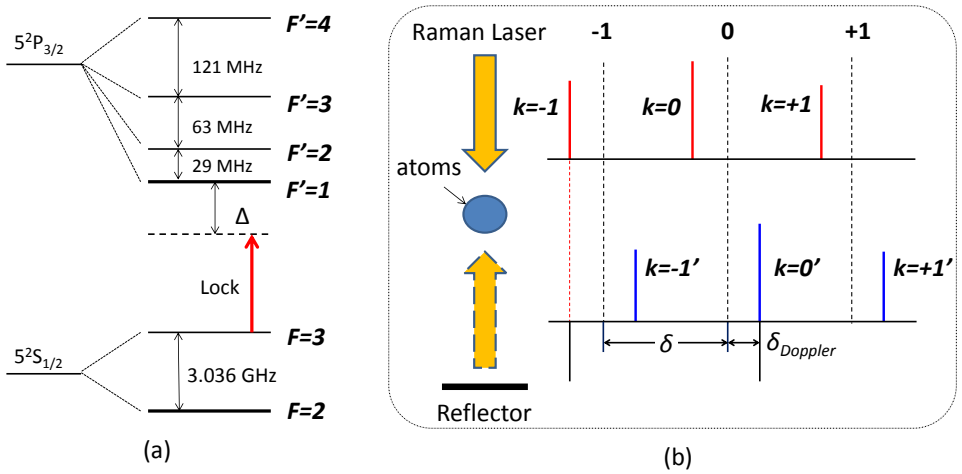

Fig. 8. (a): Hyperfine levels of ^{85}Rb D_2 transition. (b): Schematic diagram of the Raman lasers.

As is shown in Fig. 8(b), there are two pairs of Raman laser components that can simultaneously drive the Doppler-sensitive transition, e.g. $k = +1$ & $k = 0'$ and $k = 0$ & $k = -1'$ (the other option is $k = +1'$ & $k = 0$ and $k = 0'$ & $k = -1$, corresponding to opposite Doppler shift). Therefore, the effective Rabi frequency of the Doppler-sensitive Raman transition is:

$$\Omega_{eff} = \sum_{F'} \frac{\Omega_{F=2,F',k=+1} \cdot \Omega_{F=3,F',k=0'}}{4\pi \delta^{v}_{F=2,F',k=+1}} + \sum_{F'} \frac{\Omega_{F=2,F,k=0} \cdot \Omega_{F=3,F',k=-1'}}{4\pi \delta^{v}_{F=2,F',k=0}}, \quad (F' = 1,2,3,4) \tag{13}$$

Consider a vertical atom gravimeter with standard three pulse sequence $(\pi/2 - \pi - \pi/2)$, when the modulation frequency, δ, for the first $\pi/2$ pulse is 3.0357 GHz, and the corresponding SCR is 0.1445 (from the data in Fig. 4). According to Eq. (10), the detuning, Δ, is set as -2.1144 GHz to cancell the AC-Stark shift. For the last $\pi/2$ pulse, the modulation frequency δ' should be chirped as

$$\delta' = \delta + k_{eff} \cdot g \cdot 2T \tag{14}$$

Optics EXPRESS

where, k_{eff} is the effective wave vector (1.6×10^7 m^{-1} for 780 nm), g is the gravitational acceleration and T is the free evolution time between the pulses. For different Raman laser pairs, k= $+1'$ & k = 0 and k = $0'$ & k = -1 pairs or k = $+1$ & k = $0'$ and k = 0 & k = $-1'$ pairs, k_{eff} is reversed and the chirping rate is of opposite sign.

If the total intensity of Raman beams is 100 mW/cm^2, the AC-Stark shift of the last $\pi/2$ pulse for different T is calculated by Eq. (10), the results for both positive and negative chirping are shown in Fig. 9(a). Without the compensation of SCR, the AC-Stark shift varies from -6467.8 Hz to 617.9 Hz. However, as is shown in Fig. 6(a), the average variation of SCR is reduced to less than 0.1% after SCR locked, thus the maximum AC-Stark shift is calculated as 70.6 Hz.

The phase shift of the interference fringes caused by AC-Stark shift is given as [22]:

$$\Delta\phi_{AC} = \frac{\delta_3^{AC} - \delta_1^{AC}}{\Omega_{eff}} \tag{15}$$

where, δ_1^{AC} and δ_3^{AC} represent the AC-Stark shift by the first and the last $\pi/2$ Raman pulses, respectively. The induced system error of the g measurement is

$$\Delta g = \frac{\Delta\phi_{AC}}{k_{eff}\cdot T^2} \tag{16}$$

As the effective Rabi frequency, Ω_{eff}, is evaluated as 220.1 kHz by Eq. (13), the $\Delta g(T)$ corresponding to the AC-Stark shifts in Fig. 9(a) are calculated and shown in Fig. 9(b).

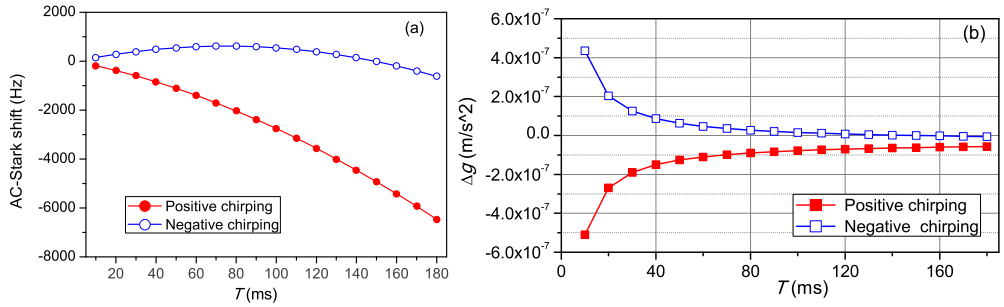

Fig. 9. (a): AC-Stark shift with different T. (b): System error for measurement of gravity with different T.

When we choose of positive chirping (with k = $+1$ & k = $0'$, k = 0 & k = $-1'$ pairs) in Fig. 9(b), for T = 180 ms, the g measurement error caused by AC-Stark shift is up to $5.7\times10^{-9}g$. Moreover, since the two curves in Fig. 9(b) are not overlapped, this error can't be rejected by known techniques. By employing the technique of SCR locking in this work, the g measurement error caused by this AC-Stark shift can be averaged down to be $6.2\times10^{-11}g$.

6. Conclusion

We proposed and demonstrated a frequency beating method and carried out accurate measurement and closed loop control of FEOM's SCR. The influence of the frequency-dependent character of the beating measurement system was largely decreased by synchronously scanning the frequency of the reference beam. Through the locking control of the SCR by feedback to the modulation depth, both the SCR variation and the corresponding measurement error can be reduced by about 2 orders. This work can provide a reference for other precision measurements involving EOMs.

Optics EXPRESS

Funding

National Key Research and Development Program of China (2016YFA0302002); National Natural Science Foundation of China (11504411, 91536221, 11304358, 11227803); Strategic Priority Research Program of the Chinese Academy of Sciences (XDB21010100).